Journal of Biomolecular NMR, **17:** 167–174, 2000.
KLUWER/ESCOM

The use of chemical shift temperature gradients to establish the paramagnetic susceptibility tensor orientation: Implication for structure determination/refinement in paramagnetic metalloproteins

Zhicheng Xia*, Bao D. Nguyen** & Gerd N. La Mar***
Department of Chemistry, University of California, Davis, CA 95616, U.S.A.

Received 7 February 2000; Accepted 20 April 2000

Key words: dipolar shift, dipolar shift temperature dependence, metalloprotein, paramagnetic susceptibility tensor, protein structure determination

Abstract

The use of dipolar shifts as important constraints in refining molecular structure of paramagnetic metalloproteins by solution NMR is now well established. A crucial initial step in this procedure is the determination of the orientation of the anisotropic paramagnetic susceptibility tensor in the molecular frame which is generated interactively with the structure refinement. The use of dipolar shifts as constraints demands knowledge of the diamagnetic shift, which, however, is very often not directly and easily accessible. We demonstrate that temperature gradients of dipolar shifts can serve as alternative constraints for determining the orientation of the magnetic axes, thereby eliminating the need to estimate the diamagnetic shifts. This approach is tested on low-spin, ferric sperm whale cyanometmyoglobin by determining the orientation, anisotropies and anisotropy temperature gradients by the alternate routes of using dipolar shifts and dipolar shift gradients as constraints. The alternate routes ultimately lead to very similar orientation of the magnetic axes, magnetic anisotropies and magnetic anisotropy temperature gradients which, by inference, would lead to an equally valid description of the molecular structure. It is expected that the use of the dipolar shift temperature gradients, rather than the dipolar shifts directly, as constraints will provide an accurate shortcut in a solution structure determination of a paramagnetic metalloprotein.

Abbreviations: metMbCN, cyanometmyoglobin; MbCO, carbonmonoxymyoglobin.

Introduction

The strong relaxation and large hyperfine shifts (Bertini and Luchinat, 1986; Kurland and McGarvey, 1970) for nuclei near the active site due to the unpaired electron spin(s) in paramagnetic metalloproteins were long considered to seriously undermine the efficacy of the 2D NMR experiments needed to assign and characterize the active site nuclei. Moreover, paramagnetic leakage leads to only minimal NOEs near the metal. Significant progress in appropriately tailored NMR to the rapid relaxation of active site residues (La Mar and de Ropp, 1993; Bertini and Luchinat, 1996), however, has shown that the 2D methods are surprisingly effective. Essentially complete assignment of active site residues of the low-spin ferric hemoproteins (La Mar et al., 1999) and iron-sulfur proteins (Bertini et al., 1999) are now routine. These methods have also been extended with some success to tackle more strongly paramagnetic environments, such as in the high-spin cytochrome c′ (Caffrey et al., 1995; Clark et al., 1996; Tsan et al., 1999). Paramagnetic relaxation (Solomon, 1955) and dipolar shifts (Kurland and McGarvey, 1970; Williams et al., 1985; Qin et al., 1993a,b; Case, 1998; Banci et al., 1999b), on the other hand, can serve as crucial structural constraints

*Present address: Department of Chemistry, McGill University, Montreal, Canada H2A 3A7.
**Present address: Department of Biochemistry and Molecular Biology, University of Georgia, Athens, GA 30602-7229, U.S.A.
***To whom correspondence should be addressed. E-mail: lamar@indigo.ucdavis.edu

that readily substitute for the conventional NOE constraints near the active site, such that solution NMR structure determination of many paramagnetic metalloproteins can be carried out essentially as effectively as for diamagnetic proteins (Feng et al., 1990; Harper et al., 1993; Gochin and Roder, 1995; Baistrocchi et al., 1996; Banci et al., 1996, 1997a,b, 1998a, 1999a; Qi et al., 1996; Bentrop et al., 1997; Assfalg et al., 1998; Turner et al., 1998). The dipolar shifts, moreover, serve as much more effective constraints of long-range order, inasmuch as they fall off as R_M^{-3} (where R_M is the distance between the nucleus and the metal), rather than as r_{ij}^{-6} (where r_{ij} is the proton-proton distance), and are therefore superior to NOEs for defining the structure of protein–protein (Guiles et al., 1996; Sukits et al., 1997; Ubbink et al., 1998), protein–DNA (Schmiedeskamp and Klevitt, 1997) or DNA–drug complexes (Gochin, 1998; Tu and Gochin, 1999).

The dipolar shift of interest, δ_{dip}, is given by (Kurland and McGarvey, 1970; Bertini and Luchinat, 1996):

$$\delta_{dip}(\text{calc}) = \frac{1}{12\pi N}\{\Delta\chi_{ax}(3\cos^2\theta - 1)R^{-3} + 3/2\Delta\chi_{rh}(\sin^2\theta\cos 2\Omega)R^{-3}\}, \quad (1)$$

where R, θ, Ω define the geometric position of a nucleus in the *magnetic coordinate system*, x, y, z, (R, θ, Ω), where the paramagnetic susceptibility tensor, χ, is diagonal, and $\Delta\chi_{ax} = \chi_{zz} - (\chi_{xx} + \chi_{yy})/2$ and $\Delta\chi_{rh} = \chi_{xx} - \chi_{yy}$. In general, neither the $\Delta\chi$s nor the orientation of the magnetic axes in the molecular frame are known and must be determined from the dipolar shifts. Hence, Equation 1 must be recast in the form (Williams et al., 1985; Emerson and La Mar, 1990):

$$\delta_{dip}(\text{calc}) = \frac{1}{12\pi N}\{\Delta\chi_{ax}(3\cos^2\theta' - 1)R^{-3} + 3/2\Delta\chi_{rh}(\sin^2\theta'\cos 2\Omega')R^{-3}\} \Gamma(\alpha, \beta, \gamma) \quad (2)$$

where R, θ', Ω' are the coordinates in some arbitrary, metal-centered, molecular reference coordinate system, x′, y′, z′, and $\Gamma(\alpha, \beta, \gamma)$ is the Euler transformation that converts the metal-centered reference coordinates into the magnetic coordinates, i.e., (x, y, z) = (x′, y′, z′)$\Gamma(\alpha, \beta, \gamma)$, where α, β, γ are the standard Euler angles. Figure 1 depicts the relationship between the two sets of coordinates in terms of the Euler angles. Thus, effective use of δ_{dip} as a structural constraint demands first determining the orientation

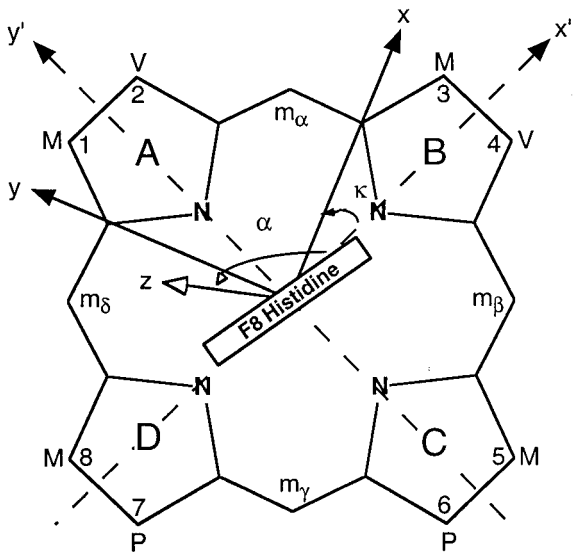

Figure 1. Definition of the magnetic axes, x, y, z, in metMbCN, based on a pseudosymmetric, iron-centered reference frame, x′, y′, z′, where z′ corresponds to the heme normal oriented toward the proximal side of the heme and x′, y′ lie in the heme plane and pass through the N_C-Fe-N_A and N_B-Fe-N_D vectors. The magnetic and reference coordinate systems are related by the standard Euler rotation, $\Gamma(\alpha, \beta, \gamma)$, where (x, y, z) = (x′, y′, z′)$\Gamma(\alpha, \beta, \gamma)$. β is the tilt of the major axes from the heme normal, α is the angle of the projection of the z axis on the x′,y′ plane with respect to the x′ axis and $\kappa = \alpha+\gamma$ corresponds approximately to the location of the rhombic magnetic axes, x,y, relative to the x′,y′ axes.

of the magnetic axes and such a determination (or minimal estimation) is intrinsic to the use of δ_{dip} to generate or refine a solution NMR structure (Banci et al., 1996, 1997c; Tu and Gochin, 1999).

The established procedure for determining α, β, γ (and, if necessary, $\Delta\chi_{ax}$, $\Delta\chi_{rh}$) is to carry out a least-squared search for the best fit between δ_{dip}(calc) via Equation 2 and δ_{dip}(obs) with $\Gamma(\alpha, \beta, \gamma)$ (and, if necessary, $\Delta\chi_{ax}$, $\Delta\chi_{rh}$) as variables, where the observed dipolar shift for non-coordinated residue nuclei is given by:

$$\delta_{dip}(\text{obs}) = \delta_{DSS}(\text{obs}) - \delta_{DSS}(\text{dia}) \quad (3)$$

δ_{DSS}(obs) is the observed shift, referenced to DSS, in the paramagnetic complex, and δ_{DSS}(dia) is the chemical shift, relative to DSS, that would be expected in an isostructural diamagnetic complex. The geometric factors in Equation 2 would be generated interactively with the solution structure determination.

One major difficulty in this approach is that δ_{DSS}(dia) values are generally not available. Estimates have to be generated either by collecting NMR spectra for a carefully chosen diamagnetic compound

with subsequent detailed assignments, or by calculations based on molecular structures (Cross and Wright, 1985; Wishart et al., 1991). The error in δ_{dip}(obs) can be very significant due to uncertainties in δ_{DSS}(dia), in particular, for nuclei relatively remote from the metal where 2D assignments are still straightforward, but dipolar shifts are no longer negligible. The approach we propose here to circumvent the lack of knowledge about δ_{DSS}(dia) is to use the temperature gradients of dipolar shifts, rather than the dipolar shifts themselves, as constraints. The exact temperature behaviors of $\Delta\chi_{ax}$ and $\Delta\chi_{rh}$ are not known, and generally differ for the two terms, with neither adhering to the simple Curie (T^{-1}) law. This has been demonstrated theoretically (Horrocks and Greenberg, 1974) and confirmed experimentally (Nguyen et al., 1999) for low-spin ferric hemoproteins. However, plots of δ_{dip} versus reciprocal temperature (Curie plots) still yield straight lines over the accessible temperature range (although non-zero interacts at $T^{-1} = 0$), and the slope of this plot is proportional to δ_{dip}, as demonstrated for low-spin ferric hemoproteins (Emerson and La Mar, 1990).

With reasonable assumptions that both the molecular structure, (R, θ, Ω), and the magnetic axes, (α, β, γ), are independent of temperature over the accessible temperature range, Equation 2 can be recast as:

$$\mathrm{Gr}(\delta_{dip}(\mathrm{calc})) = \frac{1}{12\pi N}\{\mathrm{Gr}(\Delta\chi_{ax})(3\cos^2\theta' - 1)R^{-3} + \frac{3}{2}\mathrm{Gr}(\Delta\chi_{rh})(\sin^2\theta'\cos 2\Omega')R^{-3}\}\,\Gamma(\alpha,\beta,\gamma), \quad (4)$$

with $\mathrm{Gr}(Y) = d(Y)/d(T^{-1})$ (where $Y = \delta_{dip}$(calc), $\Delta\chi_{ax}$ or $\Delta\chi_{rh}$). Similarly, Equation 3 is recast as:

$$\mathrm{Gr}(\delta_{dip}(\mathrm{obs})) = \mathrm{Gr}(\delta_{DSS}(\mathrm{obs})) - \mathrm{Gr}(\delta_{DSS}(\mathrm{dia})) \cong \mathrm{Gr}(\delta_{DSS}(\mathrm{obs})), \quad (5)$$

where $\mathrm{Gr}(X) = dX/d(T^{-1})$ (with $X = \delta_{dip}$(obs), δ_{DSS}(obs), and δ_{DSS}(dia)), and we have made the reasonable assumption that δ_{DSS}(dia) is independent of temperature (Baxter and Williamson, 1997). A least-square search (with α, β, γ, $\mathrm{Gr}(\Delta\chi_{ax})$ and $\mathrm{Gr}(\Delta\chi_{rh})$ as variables) that minimizes the differences between Equations 4 and 5 should yield $\Gamma(\alpha, \beta, \gamma)$, i.e., the magnetic axes without having to have even an estimate of δ_{DSS}(dia).

A reasonable test of the ability to generate robust magnetic axes using gradients of dipolar shifts is to carry out a determination of the magnetic axes, as well as anisotropies and anisotropy gradients, on a structurally characterized metalloprotein (where r, θ', Ω' in Equations 2 and 4 are available), where both δ_{dip}(obs) (via Equation 3 and $\mathrm{Gr}(\delta_{dip}(\mathrm{obs}))$ (via Equation 5) are available, and where the magnetic axes can be determined using the identical proton coordinates in the alternate routes. The ideal system to test this approach is sperm whale metMbCN, a low-spin, ferric hemoprotein for which extensive assignments of heme cavity residues have been reported (Emerson and La Mar, 1990; Nguyen et al., 1999), the magnetic axes have been determined over the temperature range 5–50 °C using δ_{dip}(obs) as constraints (Nguyen et al., 1999), and for which both the crystal structure (Kuriyan et al., 1986) and experimental δ_{DSS}(dia) (Theriault et al., 1994) are available for the isostructural MbCO complex. We show herein that the alternate approaches to determining the magnetic axes, the anisotropies, and the anisotropy gradients, are remarkably consistent with each other and confirm the validity of using temperature gradients of dipolar shifts as constraints for determining the magnetic axes, and by inference, suggest that the gradients can serve as structural constraints in structure determination/refinement.

Materials and methods

^1H NMR data

The δ_{DSS}(obs) for 26 non-labile protons of sperm whale metMbCN with significant δ_{dip}(obs) have been reported (Nguyen et al., 1999) over the temperature range 5–50 °C. The δ_{DSS}(obs) at 25 °C and the temperature gradients, $\mathrm{Gr}(\delta_{DSS}(\mathrm{obs}))$, obtained from excellent fits to a straight line in a δ_{DSS}(obs) vs 1/T plot over this temperature range, are listed in Table 1.

Magnetic axes determination using δ_{dip}(obs)

The magnetic axes were determined for metMbCN by carrying out a five-parameter, least-square search (Clayden et al., 1987; Emerson and La Mar, 1990; Qin et al., 1993a,b; Rajarathnam et al., 1993; Zhao et al., 1995; Zhang et al., 1997; Nguyen et al., 1999) for $\Delta\chi$s and $\Gamma(\alpha,\beta,\gamma)$ that minimizes the error function, F/n, for n(= 26) nuclei:

$$F/n(\alpha,\beta,\gamma,\Delta\chi_{ax},\Delta\chi_{rh}) = \frac{1}{n}\sum_{i=1}^{n}\left|\delta^i_{dip}(\mathrm{obs}) - \delta^i_{dip}(\mathrm{calc})\right|^2 \quad (6)$$

Table 1. ^{1}H NMR spectral data for sperm whale metMbCN

Residue	Proton	δ_{DSS}(obs)[a] (ppm)	δ_{dip}(obs)[a] (ppm)	δ_{dip}(calc)[a] (ppm)	Gr(δ_{dip}(obs))[a] (10^3 ppm K)	Gr(δ_{dip}(calc)) (10^3 ppm K)
Phe 33(B14)	$C_\delta Hs$	8.04	1.04	0.90	0.45	0.48
	$C_\epsilon Hs$	8.32	1.86	1.77	1.12	0.91
	$C_\zeta H$	8.40	3.19	3.31	1.75	1.62
Phe 43(CD1)	$C_\zeta H$	17.27	12.54	12.97	6.46	6.72
His 64(E7)	$C_\alpha H$	4.12	−0.06	0.20	0.00	−0.21
Thr 67(E10)	$C_\alpha H$	2.47	−1.37	−1.53	−0.63	−0.92
Val 68(E11)	$C_\alpha H$	−2.53	−5.79	−5.91	−3.53	−3.89
Ala 71(E14)	$C_\alpha H$	3.49	−1.13	−1.10	−0.33	−0.58
	$C_\beta H_3$	−0.15	−2.55	−2.51	−0.96	−1.37
Leu 89(F4)	$C_\alpha H$	8.64	4.90	4.74	1.79	1.68
Ala 90(F5)	$C_\alpha H$	6.47	3.03	2.99	1.39	1.28
	$C_\beta H_3$	2.64	1.47	1.46	0.73	0.62
His 93(F8)	$C_\alpha H$	7.47	4.57	4.61	1.79	1.68
His 97(FG3)	$C_\delta H$	11.01	8.67	9.52	5.06	5.09
	$C_\epsilon H$	6.81	−1.11	−0.80	−0.29	0.08
Ile 99(FG5)	$C_\alpha H$	2.34	−1.95	−2.06	−1.15	−1.24
	$C_\beta H$	−0.12	−1.49	−1.59	−1.10	−1.43
	$C_\gamma H$	−1.91	−2.29	−2.42	−1.88	−2.01
	$C_\gamma H'$	−9.60	−9.32	−9.83	−7.32	−6.50
	$C_\gamma H_3$	−3.46	−4.85	−4.56	−2.32	−2.58
	$C_\delta H_3$	−3.83	−5.30	−4.94	−2.67	−2.83
Tyr 103(G4)	$C_\delta Hs$	5.66	−1.64	−1.82	−0.62	−0.83
	$C_\epsilon Hs$	6.27	−0.93	−0.76	−0.07	−0.47
Phe 138(H15)	$C_\delta Hs$	7.01	−0.07	−0.18	0.09	−0.07
	$C_\epsilon Hs$	6.91	−0.02	−0.33	0.03	−0.14
	$C_\zeta H$	7.03	0.03	0.06	0.03	−0.01

[a]Data at 25 °C in ^1H_2O at pH 8.6 taken from (Nguyen et al., 1999).

using the MbCO crystal coordinates (Kuriyan et al., 1986) to generate θ', Ω' and R, and published δ_{DSS}(MbCO) (Theriault et al., 1994) for δ_{DSS}(dia), and Equations 2 and 3 to obtain δ_{dip}(calc) and δ_{dip}(obs), respectively, as has been reported previously (Emerson and La Mar, 1990; Nguyen et al., 1999). The arbitrary molecular coordinate system was chosen to be centered at the iron atom, with the x′, y′ axes in the heme plane, as depicted in Figure 1, which also defines the Euler angles. The values for the anisotropies and Euler angles at 25 °C that result from using Equations 2, 3 and 6 are listed in Table 2 (left hand column). The temperature gradients of the anisotropies, Gr($\Delta\chi$), were determined from the least-square fit to a straight line in the plots of $\Delta\chi_{ax}$ and $\Delta\chi_{rh}$ versus 1/T for magnetic anisotropies determined at each temperature in the range 5–50 °C, as reported previously (Nguyen et al., 1999), and are included in the left hand column of Table 2.

Magnetic axes determination using Gr(δ_{dip}(obs))

The temperature gradients of the observed shifts ($\approx$ Gr(δ_{dip}(obs)) in Equation 5) were obtained from the slopes of a plot of δ_{DSS}(obs) versus reciprocal absolute temperature over the temperature range 5–50 °C (Nguyen et al., 1999). The magnetic axes were determined by carrying out a five-parameter, least-squares search for the minimum in the error function, F*/n, in Equation 7, for n(= 26) nuclei:

$$F^*/n(\alpha, \beta, \gamma, Gr(\Delta\chi_{ax}), Gr(\Delta\chi_{rh})) = \frac{1}{n}\sum_{i=1}^{n}\left|Gr(\delta^i_{dip}(obs)) - Gr(\delta^i_{dip}(calc))\right|^2 \quad (7)$$

Table 2. Comparison of magnetic axes orientation, magnetic anisotropies and temperature gradients of magnetic anisotropies for metMbCN determined using either δ_{dip}(obs) or Gr(δ_{dip}(obs)) as constraints

	Constraints	
	δ_{dip}(obs)	Gr(δ_{dip}(obs))
Euler angles (°)		
α	143[a]	167[b]
β	15.7[a]	18.6[b]
$\kappa = \alpha + \gamma$	−9[a]	−14[b]
Anisotropies		
$\Delta\chi_{ax} \times 10^8$ (m^3/mol)	2.53[a]	2.36[c]
$\Delta\chi_{rh} \times 10^8$ (m^3/mol)	−0.64[a]	−0.32[c]
Residual F/n[d]	0.040	0.059
Anisotropy gradients		
Gr($\Delta\chi_{ax}$) × 10^5 (m^3 K/mol)	1.18[e]	1.22[b]
Gr($\Delta\chi_{rh}$) × 10^5 (m^3 K/mol)	−1.41[e]	−1.45[b]

[a]Data from (Nguyen et al., 1999), obtained via the procedures described in the first two steps of Equation 9a involving minimization of the error function in Equation 6.
[b]Data obtained here via the procedure described in the first two steps of Equation 9b involving minimization of the error function in Equation 7.
[c]Data obtained via the procedure described in the last step of Equation 9b by minimizing the error function F′/n in Equation 8, based on the α, β, γ obtained in [b] above.
[d]The units of the error functions in the two approaches are different. For the approach using dipolar shifts, the unit is in ppm^2, while for the gradient approach, the unit is in 10^{-6} ppm^2 K^2.
[e]Taken from (Nguyen et al., 1999) and obtained from plot of $\Delta\chi$s vs T^{-1} with the $\Delta\chi$s obtained by five-parameter searches at each temperature.

using the temperature gradients for the same 26 protons as input, the MbCO crystal coordinates (Kuriyan et al., 1986) to generate θ′, Ω′ and R, and Equations 4 and 5 to obtain Gr(δ_{dip}(obs)) and Gr(δ_{dip}(calc)), respectively. The resulting orientation of the magnetic axes, α, β, γ, and Gr($\Delta\chi$s) using Equations 4, 5 and 7, are presented in the right hand column of Table 2.

The anisotropies at 25 °C are subsequently estimated by a two-parameter search for the minimum in the error function, F′/n in Equation 8,

$$F'/n(\Delta\chi_{ax}, \Delta\chi_{rh}) = \frac{1}{n}\sum_{i=1}^{n}\left|\delta^i_{dip}(obs) - \delta^i_{dip}(calc)\right|^2, \quad (8)$$

using α, β, γ from the magnetic axes determined from the temperature gradients in Equation 7. The anisotropies so determined at 25 °C are included in the lower right hand side of Table 2.

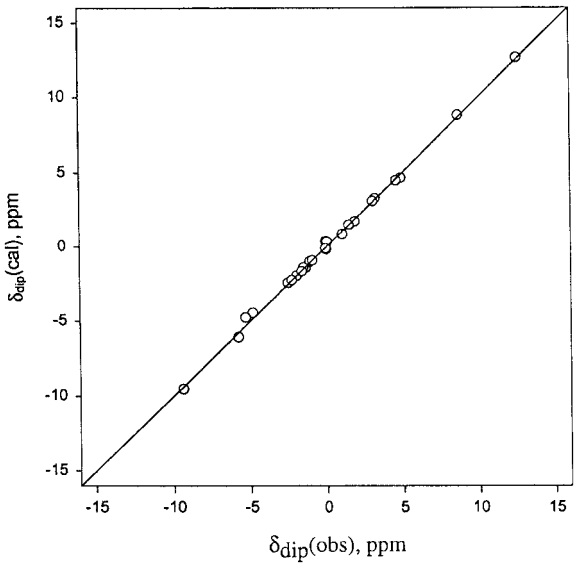

Figure 2. Plot of δ_{dip}(obs) vs δ_{dip}(calc), at 25 °C, for the optimized magnetic axes resulting from a five-parameter, least-square search for Γ(α, β, γ) and $\Delta\chi$s, based on Equations 2, 3 and 6, using δ_{dip}(obs) for 26 protons in Table 1 as constraints. The solid line corresponds to a perfect fit.

Results and discussion

Orientation of the magnetic axes

The quality of the fit between δ_{dip}(obs) (via Equation 3) and optimized δ_{dip}(calc) (via Equation 2) obtained using δ_{dip}(obs) as constraints (Nguyen et al., 1999) at 25 °C is excellent, as shown in Figure 2. The values of the three Euler angles (α, β, and $\kappa = \alpha + \gamma$) at 25 °C have been reported (Nguyen et al., 1999) and are reproduced on the left side of Table 2. Analysis of a large body of ^{1}H NMR data for metMbCN (Nguyen et al., 1999) has shown that the combined uncertainties due to selection of limited input data sets and the intrinsic uncertainties in the optimization of even the ideal, nearly complete data set, result in parameters with uncertainties of ±10° for α, ±1.5° for β, and ±10° for $\kappa = \alpha + \gamma$.

The determination of the orientation of the magnetic axes based on Gr(δ_{dip}(obs)) similarly yields an excellent fit between Gr(δ_{dip}(obs)) and Gr(δ_{dip}(calc)), as illustrated in Figure 3. The resulting Euler angles, α, β, and $\kappa = \alpha + \gamma$, are included in the right column of Table 2. Comparison of the Euler rotation angles obtained by these two alternate routes in Table 2 reveals that they are very similar. The differences are generally close to the expected uncertainties of the data sets.

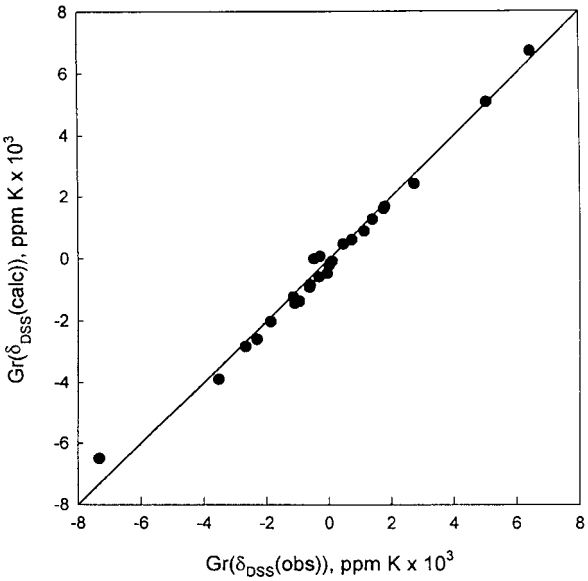

Figure 3. Plot of Gr(δ_{dip}(obs)) vs Gr(δ_{dip}(calc)) for the optimized magnetic axes resulting from a five-parameter least-square search for $\Gamma(\alpha, \beta, \gamma)$ and the Gr($\Delta\chi$)s, based on Equations 4, 5 and 7, using temperature gradients of the dipolar shifts for 26 protons in Table 1 as constraints. The solid line corresponds to a perfect fit.

The magnetic anisotropies

The values for $\Delta\chi_{ax}$ and $\Delta\chi_{rh}$ resulting from a five-parameter search based on dipolar shifts as constraints (i.e., via Equations 2, 3, and 6) have been reported and are reproduced in the left side of Table 2. The analysis of extensive NMR data on sperm whale metMbCN (Nguyen et al., 1999) has revealed that the uncertainties in the anisotropies determined in this manner are $\pm 0.15 \times 10^{-8}$ m^3/mol for $\Delta\chi_{ax}$, and $\pm 0.17 \times 10^{-8}$ m^3/mol for $\Delta\chi_{rh}$.

The anisotropies based on magnetic axes orientations determined using Gr(δ_{dip}(obs)) as constraints (i.e., Equations 4, 5 and 7) are not available from the first least-square search (Equation 7), which yields the Euler angles and anisotropy gradients. However, $\Delta\chi$s may be obtained at any temperature by minimizing the error function in Equation 8, where estimates to δ_{DSS}(dia) via Equation 3 are now necessary. The two-parameter search, using the α, β, γ values determined based on Gr(δ_{dip}(obs)), yields the anisotropies listed in the right hand column of Table 2. It is apparent in Table 2 that the values for $\Delta\chi_{ax}$ and $\Delta\chi_{rh}$ are very similar from the alternate routes to the magnetic axes, with the differences within the uncertainties of each determination.

The magnetic anisotropy gradients

The Gr($\Delta\chi_{ax}$) and Gr($\Delta\chi_{rh}$) values are obtained directly from the five-parameter search based on Equations 4, 5 and 7, and are listed in the right side of Table 2. The same parameters are obtained based on magnetic axes determinations using Equations 2, 3 and 6 at each of a wide range of temperatures, with Gr($\Delta\chi_{ax}$) and Gr($\Delta\chi_{rh}$) obtained from the slope of the straight line in a plot of $\Delta\chi$(T) versus reciprocal temperature, as reported previously (Nguyen et al., 1999). Such data covering the temperature range 5–50 °C has been reported for metMbCN, and the plots yield the anisotropy gradients which are included in the left hand column of Table 2. Comparison of the two sets of data in Table 2 shows that two anisotropy gradients obtained by the alternate approaches are essentially the same. Each of the two approaches similarly differentiates the slope of $\Delta\chi_{ax}$ and $\Delta\chi_{rh}$, with the Gr($\Delta\chi_{rh}$) much steeper (with respect to intercept of 0 at T$\rightarrow \infty$) than that for Gr($\Delta\chi_{ax}$) (Nguyen et al., 1999). The effect is expected (Horrocks and Greenberg, 1974), since there is significant thermal population of the excited $S = \frac{1}{2}$ orbital state whose $\Delta\chi_{rh}$ has about the same magnitude, but opposite sign, of that in the ground state (Banci et al., 1998b; Nguyen et al., 1999), such that the effective $\Delta\chi_{rh} \rightarrow 0$ as T $\rightarrow \infty$. The $\Delta\chi_{ax}$, in contrast, is essentially the same in the ground and excited orbital state with $S = \frac{1}{2}$ and exhibits (Nguyen et al., 1999) a temperature gradient close to the predicted (Horrocks and Greenberg, 1974) gradient.

Comparison of the two approaches to $\Gamma(\alpha, \beta, \gamma)$

Each of the seven parameters (α, β, γ, $\Delta\chi_{ax}$, $\Delta\chi_{rh}$, Gr($\Delta\chi_{ax}$), and Gr($\Delta\chi_{rh}$)) obtained, provides insight into the heme cavity molecular and electronic structure not readily determined by other techniques (Shulman et al., 1971; Horrocks and Greenberg, 1974; Banci et al., 1998b; Shokhirev and Walker, 1998; Nguyen et al., 1999). The conventional (Equation 9a) and our proposed alternate (Equation 9b) routes to these parameters are summarized below:

$$\delta_{DSS}(\text{obs}) \xrightarrow{\delta_{DSS}(\text{dia})} \delta_{dip}(\text{obs}) \xrightarrow{\text{LSS}} \Delta\chi\text{s}, \Gamma(\alpha, \beta, \gamma) \xrightarrow{\text{VT}} \text{Gr}(\Delta\chi\text{s}) \tag{9a}$$

$$\delta_{DSS}(\text{obs}) \xrightarrow{\text{VT}} \text{Gr}(\delta_{dip}(\text{obs})) \xrightarrow{\text{LSS}} \text{Gr}(\Delta\chi\text{s}), \Gamma(\alpha, \beta, \gamma) \xrightarrow{\delta_{DSS}(\text{dia})} \Delta\chi\text{s} \tag{9b}$$

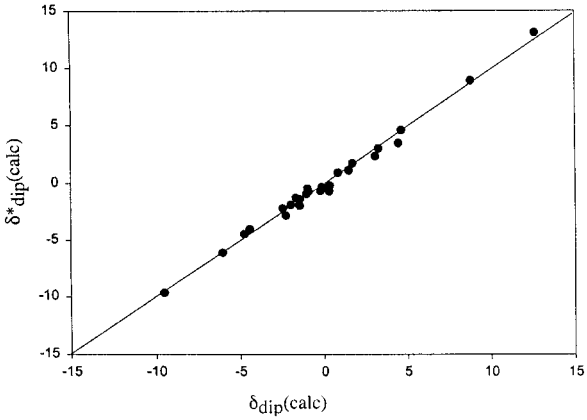

Figure 4. Plot of δ_{dip}(calc) determined by the 'conventional' procedure for determining magnetic axes (Equation 9a), versus $\delta*_{dip}$(calc) obtained using temperature gradients to determine magnetic axes, as described by Equation 9b.

where LSS and VT indicate least-square search and variable temperature, respectively.

A reasonable test of the validity of determining the orientation of the magnetic axes using solely temperature gradients is that, when using the same structural information (coordinates, δ_{DSS}(dia)), the same seven parameters are generated as when using dipolar shift as constraints. Thus Table 2 validates the route to the parameters described in Equation 9b. Lastly, the small difference in the orientation and anisotropies between the two routes largely offset each other, with the result that the predicted dipolar shifts for the individual protons obtained by these alternate routes are essentially identical, as shown in Figure 4.

The small differences in parameters observed in Table 2 may result from the different assumptions used in the two approaches. On the one hand, δ_{DSS}(dia) in Equation 3 may not exactly equal the shift in MbCO (Theriault et al., 1994). On the other hand, Equation 5 assumes that both the orientation of the magnetic axes and molecular structure are independent of temperature and that $Gr(\delta_{DSS}(dia)) = 0$. In fact, $Gr(\delta_{DSS}(dia))$ is not zero (Baxter and Williamson, 1997), but still a factor >10 smaller than $Gr(\delta_{DSS}(obs))$ for the 26 protons in metMbCN. The Euler angles, α, β, γ, have been found essentially the same within the experimental uncertainties (Nguyen et al., 1999) over the temperature range 5–50 °C. The crystal coordinates of MbCO (Kuriyan et al., 1986) may not be the same as for metMbCN, although such a difference would similarly influence both approaches to obtaining $\Gamma(\alpha, \beta, \gamma)$.

Thus there is no a priori basis for expecting either one of the approaches in Equation 9 to provide a more 'realistic' description of the magnetic axes or molecular structure. The fact that these two approaches yield essentially the same description of the magnetic properties and molecular structure underlines the conclusion that the approach should be selected on the basis of the information available. However, if δ_{DSS}(dia) were not available, the route in Equation 9b would be the choice.

Implication for molecular structure determination/refinement

Any structure determination/refinement using δ_{dip} as constraints by the route described in Equation 9a has as one of the key steps the definition of the orientation of the magnetic axes, which depends on robust estimates to δ_{DSS}(dia) (via Equation 3) to quantify δ_{dip}(obs). Uncertainties in δ_{DSS}(dia) can introduce unacceptable errors in the deduced δ_{dip}(obs) (via Equation 3), particularly for nuclei experiencing δ_{dip} comparable to shift changes induced by secondary structure (Wishart et al., 1991). The route to $\Gamma(\alpha, \beta, \gamma)$ using $Gr(\delta_{DSS}(obs))$ as constraints (Equation 9b) provides a robust magnetic axes orientation (see Table 2) without a need to address δ_{DSS}(dia). Hence, the advantage of using temperature gradient instead of the dipolar shift as constraints is obvious. In fact, δ_{DSS}(dia) needs to be determined in the last step of Equation 9b only when the anisotropies, $\Delta\chi_{ax}$ and $\Delta\chi_{rh}$, are desired.

The fact that the dipolar shift gradients generate essentially the same magnetic axes as obtained using dipolar shifts indicates that the former can also be used as constraints to determine or refine a molecular structure. Application of dipolar shifts to structural determination of paramagnetic metalloproteins has invariably led to improved definition of active site residues and a more precise location of the metal center (Banci et al., 1999b). Energy terms that include $|\delta_{dip}(obs) - \delta_{dip}(calc)|^2$ have been successfully incorporated into the computational procedures (Assfalg et al., 1998; Banci et al., 1999b; Tu and Gochin, 1999), which require at least initial estimates of δ_{DSS}(dia). It is reasonable to expect that this term can be substituted by $|Gr(\delta_{dip}(obs)) - Gr(\delta_{dip}(calc))|^2$ which completely eliminates the need for δ_{DSS}(dia) in a solution NMR structure determination.

The present work thus establishes that the magnetic axes, and by inference, the molecular structure,

can be determined without knowledge of δ_{DSS}(dia). It is expected that the use of temperature gradient will be of significant aid in refining solution structures of paramagnetic metalloproteins by ^{1}H NMR.

Acknowledgements

This research was supported by grants from the National Institutes of Health, GM26226 and HL16087.

References

Assfalg, M., Banci, L., Bertini, I., Bruschi, M. and Turano, P. (1998) *Eur. J. Biochem.*, **256**, 261–270.

Baistrocchi, P., Banci, L., Bertini, I. and Turano, P. (1996) *Biochemistry*, **35**, 13788–13796.

Banci, L., Bertini, I., Bren, K.L., Cremonini, M.A., Gray, H.B., Luchinat, C. and Turano, P. (1996) *J. Biol. Inorg. Chem.*, **1**, 117–126.

Banci, L., Bertini, I., De la Rosa, M.A., Koulougliotis, D., Navarro, J.A. and Walter, O. (1998a) *Biochemistry*, **37**, 4831–4843.

Banci, L., Bertini, I., Ferroni, F. and Rosato, A. (1997a) *Eur. J. Biochem.*, **249**, 270–279.

Banci, L., Bertini, I., Gray, H.B., Luchinat, C., Reddig, T., Rosato, A. and Turano, P. (1997b) *Biochemistry*, **36**, 9867–9877.

Banci, L., Bertini, I., Huber, J.G., Spyroulias, G.A. and Turano, P. (1999a) *J. Biol. Inorg. Chem.*, **4**, 21–31.

Banci, L., Bertini, I., Luchinat, C., Pieratetlli, R., Shokhirev, N.V. and Walker, F.A. (1998b) *J. Am. Chem. Soc.*, **120**, 8472–8479.

Banci, L., Bertini, I., Luchinat, C. and Turano, P. (1999b) In *The Porphyrin Handbook*, Vol. 5 (Kadish, K.M., Smith, K.M. and Guilard, R., Eds.), Academic Press, New York, NY, pp. 323–350.

Banci, L., Bertini, I., Savellini, G.G., Romagnoli, A., Turano, P., Cremonini, M.A., Luchinat, C., and Gray, H.B. (1997c) *Protein Struct. Funct. Genet.*, **29**, 68–76.

Baxter, N.J. and Williamson, M.P. (1997) *J. Biomol. NMR*, **9**, 359–369.

Bentrop, D., Bertini, I., Cremonini, M.A., Forsen, S., Luchinat, C. and Malmendal, A. (1997) *Biochemistry*, **36**, 11605–11618.

Bertini, I. and Luchinat, C. (1986) *NMR of Paramagnetic Molecules in Biological Systems*, Benjamin/Cummings, Menlo Park, CA.

Bertini, I. and Luchinat, C. (1996) *Coord. Chem. Rev.*, **150**, 1–296.

Bertini, I., Luchinat, C. and Rosato, A. (1999) *Adv. Inorg. Chem.*, **47**, 251–282.

Caffrey, M., Simorre, J.-P., Brutscher, B., Cusanovich, M. and Marion, D. (1995) *Biochemistry*, **34**, 5904–5912.

Case, D.A. (1998) *Curr. Opin. Struct. Biol.*, **8**, 624–630.

Clark, K., Dugad, L.B., Bartsch, R.G., Cusanovich, M.A. and La Mar, G.N. (1996) *J. Am. Chem. Soc.*, **118**, 4654–4664.

Clayden, N.J., Moore, G.R. and Williams, G. (1987) *Metal Ions Biol. Syst.*, **21**, 187–227.

Cross, K.J. and Wright, P.E. (1985) *J. Magn. Reson.*, **64**, 220–231.

Emerson, S.D. and La Mar, G.N. (1990) *Biochemistry*, **29**, 1556–1566.

Feng, Y., Roder, H. and Englander, S.W. (1990) *Biochemistry*, **29**, 3494–3504.

Gochin, M. (1997) *J. Am. Chem. Soc.*, **119**, 337.

Gochin, M. (1998) *J. Biomol. NMR*, **12**, 243–257.

Gochin, M. and Roder, H. (1995) *Protein Sci.*, **4**, 296–305.

Guiles, R.D., Sarma, S., Digate, R.J., Banville, D., Basus, V.J., Kuntz, I.D. and Waskell, L. (1996) *Nature*, **3**, 333–339.

Harper, L.V., Amann, B.T., Vinson, V.K. and Berg, J.M. (1993) *J. Am. Chem. Soc.*, **115**, 2577–2580.

Horrocks, W.D., Jr. and Greenberg, E.S. (1974) *Mol. Phys.*, **27**, 993–999.

Kuriyan, J., Wilz, S., Karplus, M. and Petsko, G.A. (1986) *J. Mol. Biol.*, **192**, 133–154.

Kurland, R.J. and McGarvey, B.R. (1970) *J. Magn. Reson.*, **2**, 286–301.

La Mar, G.N. and de Ropp, J. (1993) In *Biological Magnetic Resonance* Vol. 12 (Berliner, L.J. and Reuben, J., Eds.), Plenum Press, New York, NY, pp. 1–78.

La Mar, G.N., Satterlee, J.D. and de Ropp, J.S. (1999) In *The Porphyrin Handbook*, Vol. 5 (Kadish, K.M., Guilard, R. and Smith, K.M., Eds.), Academic Press, New York, NY, pp. 185–298.

Nguyen, B.D., Xia, Z., Yeh, D.C., Vyas, K., Deaguero, H. and La Mar, G.N. (1999) *J. Am. Chem. Soc.*, **121**, 208–217.

Qi, P.X.R., Beckman, R.A. and Wand, A.J. (1996) *Biochemistry*, **35**, 12275–12286.

Qin, J., La Mar, G.N., Ascoli, F. and Brunori, M. (1993a) *J. Mol. Biol.*, **231**, 1009–1023.

Qin, J., La Mar, G.N., Cutruzzola, F., Travaglini Allocatelli, C., Brancaccio, A. and Brunori, M. (1993b) *Biophys. J.*, **65**, 2178–2190.

Rajarathnam, K., Qin, J., La Mar, G.N., Chiu, M.L. and Sligar, S.G. (1993) *Biochemistry*, **32**, 5670–5680.

Schmiedeskamp, M. and Klevitt, R.E. (1997) *Biochemistry*, **36**, 14003–14001.

Shokhirev, N.V. and Walker, F.A. (1998) *J. Biol. Inorg. Chem.*, **3**, 581–594.

Shulman, R.G., Glarum, S.H. and Karplus, M. (1971) *J. Mol. Biol.*, **57**, 93–115.

Solomon, I. (1955) *Phys. Rev.*, **99**, 559–565.

Sukits, S.F., Erman, J.E. and Satterlee, J.D. (1997) *Biochemistry*, **36**, 5251–5259.

Theriault, Y., Pochapsky, T.C., Dalvit, C., Chiu, M.L., Sligar, S.G. and Wright, P.E. (1994) *J. Biomol. NMR*, **4**, 491–504.

Tsan, P., Caffrey, M., Daku, M.C., Cusanovich, M., Marion, D. and Gans, P. (1999) *J. Am. Chem. Soc.*, **121**, 1795.

Tu, K. and Gochin, M. (1999) *J. Am. Chem. Soc.*, **121**, 9276–9285.

Turner, D.L., Brennen, L., Chamberlin, S.G., Louro, R.O. and Xavier, A.V. (1998) *Eur. Biophys. J.*, **27**, 367–375.

Ubbink, M., Ejdeback, M., Karlsson, B.G. and Bendall, D.S. (1998) *Structure*, **6**, 323–335.

Williams, G., Clayden, N.J., Moore, G.R. and Williams, R.J.P. (1985) *J. Mol. Biol.*, **183**, 447–428.

Wishart, D.S., Sykes, B.D. and Richards, F.M. (1991) *J. Mol. Biol.*, **222**, 311–333.

Zhang, W., Cutruzzolá, F., Travaglini Allocatelli, C., Brunori, M. and La Mar, G.N. (1997) *Biophys. J.*, **73**, 1019–1030.

Zhao, X., Vyas, K., Nguyen, B.D., Rajarathnam, K., La Mar, G.N., Li, T., Phillips Jr., G.N., Eich, R.F., Olson, J.S., Ling, J. and Bocian, D.F. (1995) *J. Biol. Chem.*, **270**, 20763–20774.